https://arabjchem.org

ScientificScholar®
Knowledge is power
Publisher of Scientific Journals

Arabian Journal of Chemistry

Article in Press

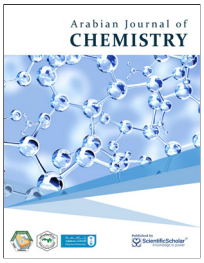

Original article

Study on the explosion suppression characteristics of typical explosion suppressants on different types of coal

Yansong Zhang[a], Yunkuan Zhang[a], Xiangbao Meng[a], Jie Zhang[b], Xiangrui Wei[a], Jing Shi[a,*]

[a] College of Safety and Environmental Engineering, Shandong University of Science and Technology, Qingdao, Shandong 266590, China
[b] College of Safety Science and Engineering, Xi'an University of Science and Technology, Xi'an 710054, China

ARTICLE INFO

Keywords:
Dust explosion
Explosion suppressant
Explosive flame
Inhibition mechanism

ABSTRACT

In response to the research problem of the lack of typical explosion suppressants on the suppression of different volatile components and fixed carbon coal dust, we studied the differences in the explosion characteristics and flame propagation characteristics of four different typical explosion suppressants on different coal dust explosion characteristics. Research has shown that sodium bicarbonate ($NaHCO_3$) and ammonium dihydrogen phosphate ($NH_4H_2PO_4$) explosion suppressants have better explosion suppression effects on long-flame coal than brown coal, whereas cyanuric acid melamine explosion suppressant has comparable explosion suppression effects on the both types of coal. The explosion suppression effect of melamine polyphosphate (MPP) is higher than the other three types of explosion suppressants. Explosion suppressants can consume high-energy free radicals such as O, OH, and H through endothermic cooling or decomposition, reducing the explosion temperature and chain reaction process.

1. Introduction

Explosions caused by coal dust pose significant risks [1-3]. When a concentrated cloud of coal dust powder cloud is ignited by energy in a confined space, it can create explosion mishaps that may even cause casualties [4-6]. Preventing coal dust explosions is a critical issue that urgently needs to be addressed.

Currently many studies focus on coal dust explosions [7-9]. Tan *et al.* studied the characteristics of coal dust explosions using a 20 L spherical explosive device and investigated the combustion and explosion reaction mechanisms from the perspective of individual dust particles [10]. They identified that the uncontrolled combustion and explosion process of coal powder in a confined space can be divided into four stages: water evaporation, volatile matter generation, volatile matter combustion, and the formation of residue and gas after combustion. Wang *et al.* explored the explosion characteristics of methane/coal dust explosions and the spatiotemporal evolution of flame flow fields by testing explosion pressure, schlieren patterns, and other factors [11]. Wang *et al.* conducted in-depth research on the influence of different ignition delays on the explosion characteristics of coal dust [12]. Experimental data shows that the explosive power reaches its peak when the ignition delay is 60 ms. Proust used transparent vertical glass tubes to study the effect of glass tube size on the propagation of dust combustion flames [13]. Since 1949, coal mine accidents that have caused more than 100 casualties in 25 incidents, coal dust explosion and gas coal dust explosion accounted for 13 of them, resulting in an average of 175 deaths per accident [14]. These alarming statistics highlight the significant threat that coal dust explosion accidents and gas coal dust explosion accidents pose to coal mine safety. The risk of coal dust explosion has become a severe challenge that urgently needs to be overcome in the coal mining industry [15]. Effectively suppressing coal dust explosions is of immeasurable importance in significantly reducing and preventing the hazards of such catastrophic accidents.

One common and effective approach for suppressing coal dust explosions is the use of inert materials [16-18]. Agar was utilized by [19] to create a composite inhibitor of urea and zeolite that primarily modifies the absorption and heat transmission among coal particles. Green waste molecular sieve-based inhibitors were utilized by [20] in order to suppress coal dust explosions through chemical and physical reactions. Jiang *et al.* revealed the key inhibitory reactions of phosphorus containing inert substances in different temperature ranges through experiments on suppressing coal dust explosions using dimethyl phosphate water mist [21]. Wei *et al.* prepared a new type of molecular sieve explosion suppressant with high thermal stability and good explosion suppression effect through experiments on suppressing coal powder explosions [22]. A lignin-based explosion suppressant was created by [23], who also examined how the features of coal dust explosions changed before and after the suppressant were added. Sun *et al.* established a directional explosion suppression model for $NaHCO_3$/coal powder and conducted explosion suppression experiments with different concentrations and particle sizes [24]. Their results showed that coal dust loss and heat release rates were lowered by $NaHCO_3$ endothermic decomposition. According to current studies, chemical powder explosion suppressants significantly suppress dust explosions [25,26]. However, most of the research focuses on the development of new explosion suppressants [27,28], lacking research on the inhibition of different volatile components and fixed carbon coal dust by typical explosion suppressants. Therefore, the effects of four different typical

***Corresponding author.**
E-mail address: shijing79516@163.com (J. Shi)

Received: 11 September, 2024 **Accepted:** 26 November, 2024 **Epub Ahead of Print:** 10 March 2025 **Published:** ***
DOI: 10.25259/AJC_15_2024

explosion suppressants—$NaHCO_3$, $NH_4H_2PO_4$, melamine cyanurate (MCA), and melamine polyphosphate (MPP)—on the explosion characteristics of lignite and long-flame coal dust are compared and studied in this article.

2. Materials and Methods

2.1. Experimental materials

Two coal types—long-flame coal from Shangwan coal mine and lignite from Baiyinhua coal mine—with varying levels of metamorphism were chosen as experimental coal samples, and screened using a standard sieve of 200 mesh (75 μm). For the purpose of suppressing coal dust flame propagation, four typical and commonly used explosive suppressants were chosen for the trials: $NaHCO_3$, $NH_4H_2PO_4$, MCA, and MPP. The particle size test results of the material are shown in Table 1.

In order to have a better understanding of the degree of deterioration and differences between the two types of coal dust, they were analyzed using a fully automatic industrial analyzer and an organic element analyzer. The analysis results are listed in Table 2. Among them, the volatile content of lignite is relatively high, reaching 39.55%, while the fixed carbon content of long-flame coal is relatively high, at 59.63%. Elemental analysis also shows that long-flame coal has a high carbon content of up to 70.35%. Therefore, the two types of coal dust selected in the experiment have significant differences and have certain research value.

2.2. Experimental methods

A 20 L nearly spherical explosion testing system and a Hartmann flame propagation testing system were used to examine the impact of four different types of explosive suppressants on the explosion properties of two different types of coal dust. The testing systems are shown in Figures 1 and 2 [29,30]. The test methods refer to EN 14034, GB/T 16426-1996, and GB/T 16428-1996 [31,32]. In the study of explosion characteristics, the concentration of powder and dust cloud is 250 g/m^3. Before the experiment, the coal powder is placed in the powder storage bin, the explosion tank is evacuated to -0.06 MPa, and the gas storage tank is filled with 2 MPa air. When the power is turned on, air will blow coal powder into the explosion tank to form a dust cloud. After a delay of 60 ms, an electric spark will be triggered to ignite the dust cloud to explode, and the data will be automatically transmitted to the computer. The Hartmann flame propagation test is similar to the above steps, except that the Hartmann device is a semi open space that does not require vacuum pumping and only requires powder spraying to delay ignition.

3. Results and Discussion

3.1. Experimental study on explosion flame propagation

It is determined from Figure 3 that the P_{max} value of long-flame coal is 0.68 MPa and that of lignite is 0.71 MPa without the addition of an explosion suppressor. Although the volatile component content of the two varies significantly, P_{max} varies within an approximate range of 0.07 MPa The high-solid carbon content of long-flame coal leads to the production of CO_2/CO during combustion, releasing a significant amount of heat energy to compensate for the insufficient maximum explosion pressure caused by low volatility. As shown in Figure 4, there is a significant difference in the $(dP/dt)_{max}$ between the two, with a difference of 3.9 MPa/s, at 24.5 MPa/s and 20.6 MPa/s, respectively. It is clearly understood that $(dP/dt)_{max}$ has a high sensitivity to the concentration of volatile components. The volatile matter content directly influences the rate and severity of coal dust explosions. For long-flame coal, lignite has an earlier starting point and reaches the maximum explosion pressure faster, resulting in a higher $(dP/dt)_{max}$ value.

It can be concluded that the addition of MPP has a greater inhibitory effect on P_{max} than other powders. As shown in Figure 5, the $(dP/dt)_{max}$ of lignite reduced to 21.9 MPa/s, 19.3 MPa/s, 15.4 MPa/s, and 7.73 MPa/s, respectively, with a decrease of 10.6%, 21.2%, 37.1%, and 68.4% by adding equal amounts of $NaHCO_3$, $NH_4H_2PO_4$, MCA, and MPP. By adding equal amounts of $NaHCO_3$, $NH_4H_2PO_4$, MCA, and MPP, the $(dP/dt)_{max}$ of long-flame coal decreased to 19.3 MPa/s, 14.2 MPa/s, 18.0 MPa/s, and 11.6 MPa/s, respectively, with a decrease of 6.3%, 31.1%, 12.6%, and 43.6%. On comparing the effectiveness of the same explosion suppressant in suppressing various volatile components of coal powder explosions, it is understood that $NaHCO_3$ exhibits a significant effect in inhibiting the $(dP/dt)_{max}$ of lignite. This is mainly attributed to the high volatile components in lignite, where $NaHCO_3$ decomposes and releases heat energy, forming free radicals such as Na, NaO, and Na_2O, which can quickly neutralize OH · and H ·, while also reducing the temperature of the gas-phase reaction environment. The $(dP/dt)_{max}$ of long-flame coal is significantly inhibited by $NH_4H_2PO_4$.

Table 1. Sample size test results.

Sample	Long-flame coal	Lignite	$NaHCO_3$	NH_4H2PO_4	MCA	MPP
D50	44.431	32.414	7.392	4.614	2.455	4.488
D[3,2]	30.627	23.546	3.294	2.306	1.749	2.377

MCA: Melamine cyanurate, MPP: melamine polyphosphate.

Table 2. Industrial and elemental analysis.

Sample	Industrial analysis (wt%, ad)				Elemental analysis (wt%, ad)				
	M_{ad}	A_{ad}	V_{daf}	FC_{ad}	C	H	N	O*	S
Shangwan Changyan Coal	6.7	5.03	26.64	61.63	70.35	4.41	1.01	23.92	0.31
Baiyinhua lignite	12.28	7.93	39.55	42.24	56.24	4.47	1.22	37.47	0.60

O * is calculated by the difference. M_{ad}: Moisture, A_{ad}: Ash, V_{daf}: Volatiles, FC_{ad}: Fixed carbon.

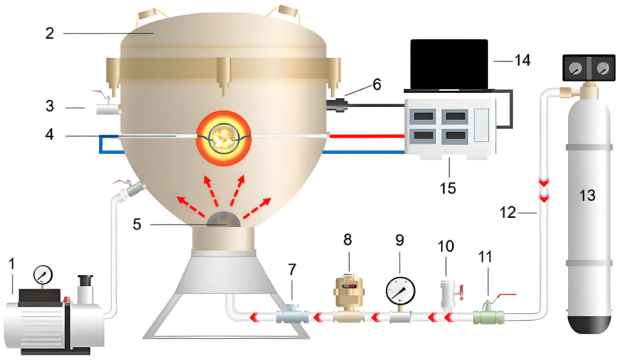

(1) Vacuum pump; (2) 20L explosion tank; (3) Exhaust valve I; (4) Ignition electrode; (5) Dust diffuser; (6) Pressure sensor; (7) Dust chamber; (8) Solenoid valve; (9) Gasholder; (10) Exhaust valve; (11) Inlet vahve; (12) Highpressure gas pipe; (13) Highpressure air tank; (14)Computer; (15) Explosion test system

Figure 1. Schematic of the 20L nearly spherical explosion testing system.

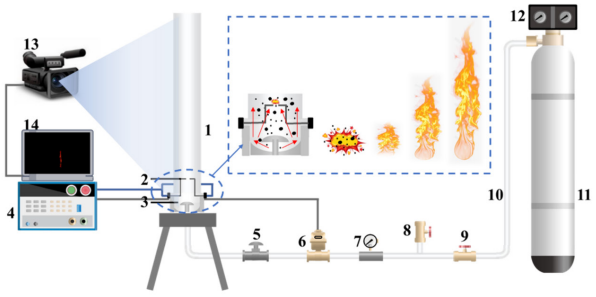

(1) Vertical glass tube; (2) Ignition electrode; (3) Dust diffuser; (4) Console; (5) Powder loading port; (6) Solenoid valve; (7) Storage tanks; (8) Exhaust valve; (9) Inlet valve; (10) High-pressure gas pipe; (11) High-pressure air cylinder; (12) Pressure gauge; (13) High-speed camera; (14) Computer

Figure 2. Diagram of Hartmann tube experimental device.

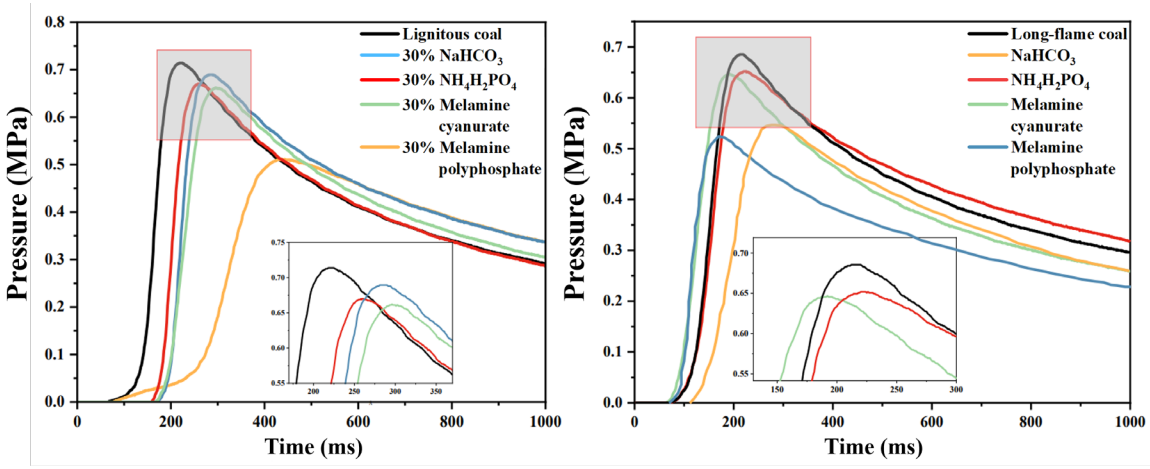

Figure 3. Effects of different explosion suppressors on two kinds of coal dust explosion pressures.

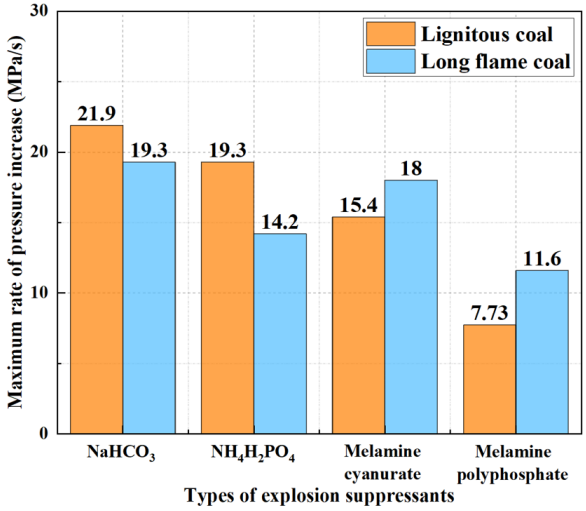

Figure 4. Maximum rate of pressure increase.

The P_{max} of lignite dropped to 0.68 MPa, 0.64 MPa, 0.61 MPa, and 0.51 MPa, respectively, when $NaHCO_3$, $NH_4H_2PO_4$, MCA, and MPP were uniformly added. This was observed when comparing the explosion pressure data of coal powder with different volatile matter contents when treated with the same explosion suppressant. The degree of reduction compared to the samples without addition was 4.2%, 9.8%, 14.1%, and 28.1%, respectively. Under the same conditions, for long-flame coal, the reduction in P_{max} is 19.1%, 5.8%, 5.3%, and 23.5%, respectively. On comparing lignite with long-flame coal, $NaHCO_3$ has a greater inhibitory effect on the pace at which lignite's P_{max} increases, but its inhibitory effect on maximum explosion pressure is not significant. In addition, $NH_4H_2PO_4$, MCA, and MPP all have better inhibitory effects on the P_{max} of lignite. Low decomposition temperature of $NaHCO_3$ plays a major role in the volatilization analysis stage, reducing the reaction temperature, while the combustion of volatile components in lignite plays a dominant role, thus reducing the maximum explosive pressure rise rate.

3.2. Analysis of explosive remnants

The scanning electron microscope (SEM) images taken before and after the coal dust explosion are shown in Figure 6. The red box represents the smooth surface of coal dust, and the red circle represents the surface holes after coal dust explosion. Prior to the explosion, the coal dust particles had a smooth surface, distinct edges, and varied sizes prior to the explosion, forming irregular block-like structures. After the explosion, dense pores can be seen on the surface of the solid coal dust residue left, and the degree of fragmentation is relatively visible. This could be due to the result of the high temperatures at which coal dust particles thermally decompose, producing volatile gases such as CO_2 and CH_4 inside. These gasses accumulate and expand collectively, fracturing the surface of the coal dust particles and creating numerous pores.

Figure 7(a-d) compares the morphology and microstructure of coal dust solid residues after adding $NaHCO_3$, $NH_4H_2PO_4$, MCA, and MPP. Among them, the red circle represents the surface pores after coal dust

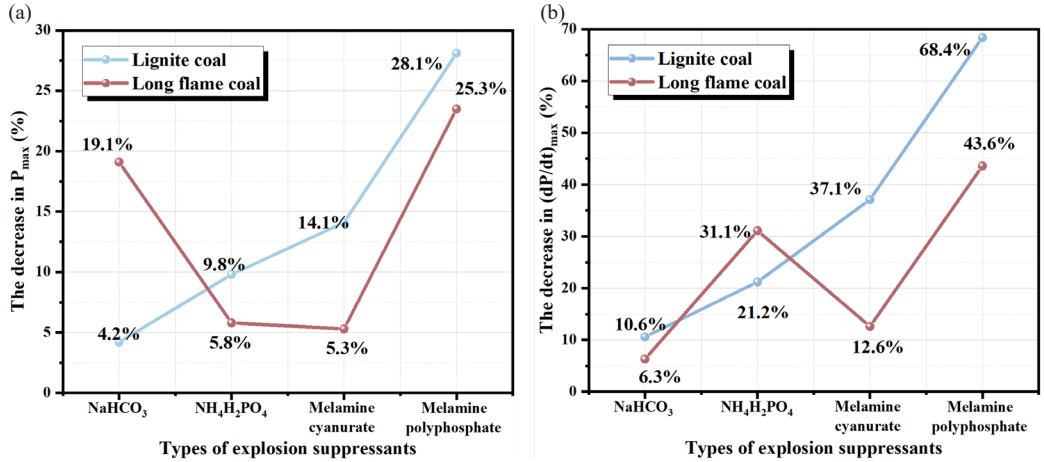

Figure 5. The reduction amplitude of the (a) P_{max} and (b) $(dP/dt)_{max}$ of coal dust under different suppression conditions.

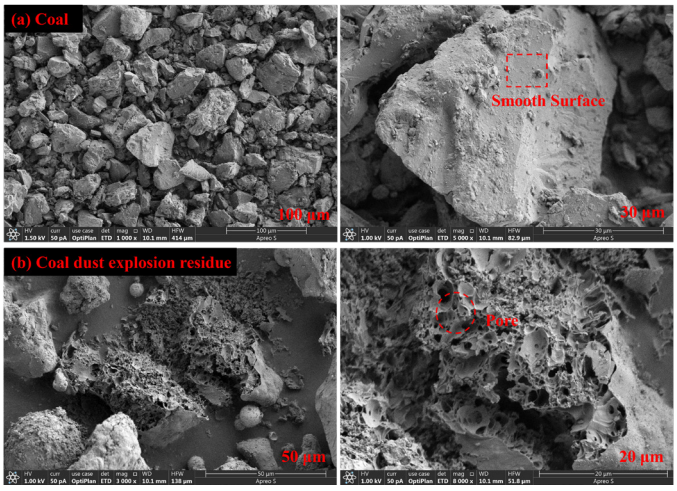

Figure 6. Scanning electron microscope (SEM) images (a) before and (b) after pure coal dust explosion.

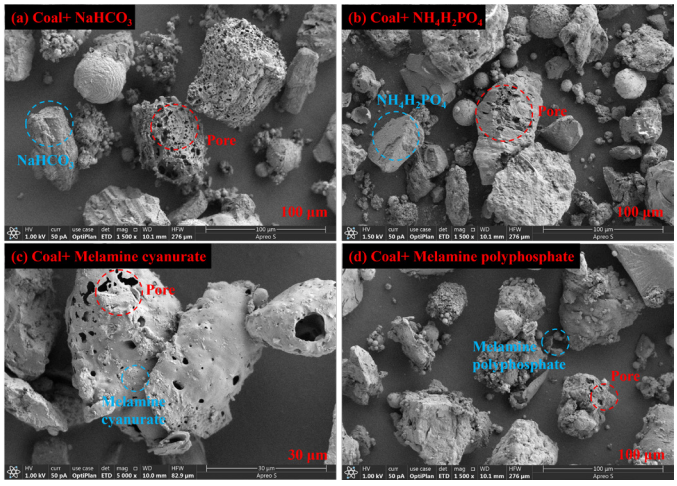

Figure 7. (a-d) Scanning electron microscope (SEM) image of residual coal dust explosion after adding explosion suppressant.

explosion, and the blue circle represents inert explosion suppressants. After adding $NaHCO_3$, the explosion suppression effect is minimal, and volatile gases are released from the thermal decomposition of coal dust, with more surface pores. After adding $NH_4H_2PO_4$, MCA, and MPP, although there are some pores on the surface of coal powder particles, the original shape is basically maintained, and the surface is relatively smooth. Comprehensive and comparative analysis of the surface microstructure of solid particles before and after coal powder explosion suppression found that the addition of explosion suppressants significantly reduced the typical explosion characteristics on the surface of the explosion solid products, indicating that the addition of explosion suppressants prevented some coal powder particles from participating in the explosion.

Infrared radiation can achieve the purpose of distinguishing molecules by illuminating the vibration frequencies of different molecular structures. Infrared spectroscopy is used to study different molecular structures and chemical bond compositions the green dashed circle represents the absorption peak. Figure 8 shows the infrared spectra of explosion products under the action of coal dust and four types of explosion suppressants. Under the action of explosion suppressants, there are certain differences in the absorption peaks of explosive products. The infrared spectra of coal and $NaHCO_3$ explosion products show a weak absorption peak at a wave number of 2880 cm^{-1}, corresponding to the C-H bond, and multiple absorption peaks at 1000–800 cm^{-1}, corresponding to NaOH lattice vibration. The explosion products of coal and $NH_4H_2PO_4$ exhibit P-O-C stretching vibration absorption peaks between 1750 and 1300 cm^{-1}. Coal and MCA explosion products exhibit N-H symmetric stretching vibration absorption peaks at 3340 cm^{-1}, and multiple stretching vibration absorption peaks between 1750 and 1300 cm^{-1}, corresponding to -NH3 deformation vibration peaks. The infrared spectra of coal and MPP explosion products are similar to $NH_4H_2PO_4$. The above analysis indicates that after adding explosion suppressants, these functional groups participate in the explosion process and play a certain role in explosion suppression.

3.3. Experimental study on the propagation of coal dust explosion flame by explosion suppressants

3.3.1. Analysis of coal powder flame morphology under different suppression conditions

Figure 9 shows that without the addition of explosion suppressants, the detonation flame of long-flame coal is brighter than that of brown coal. After ignition, long-flame coal produces a bright flame that spreads rapidly, reaches the top of the pipeline in 150 ms, while brown coal takes 250 ms to reach the top of the pipeline. Long-flame coal is stronger than brown coal in terms of flame brightness and flame speed. After adding 5% $NaHCO_3$, the flame brightness of long-flame coal significantly decreased, and the initial flame shape became more dispersed. However, after the flame fully develops, the flame is more

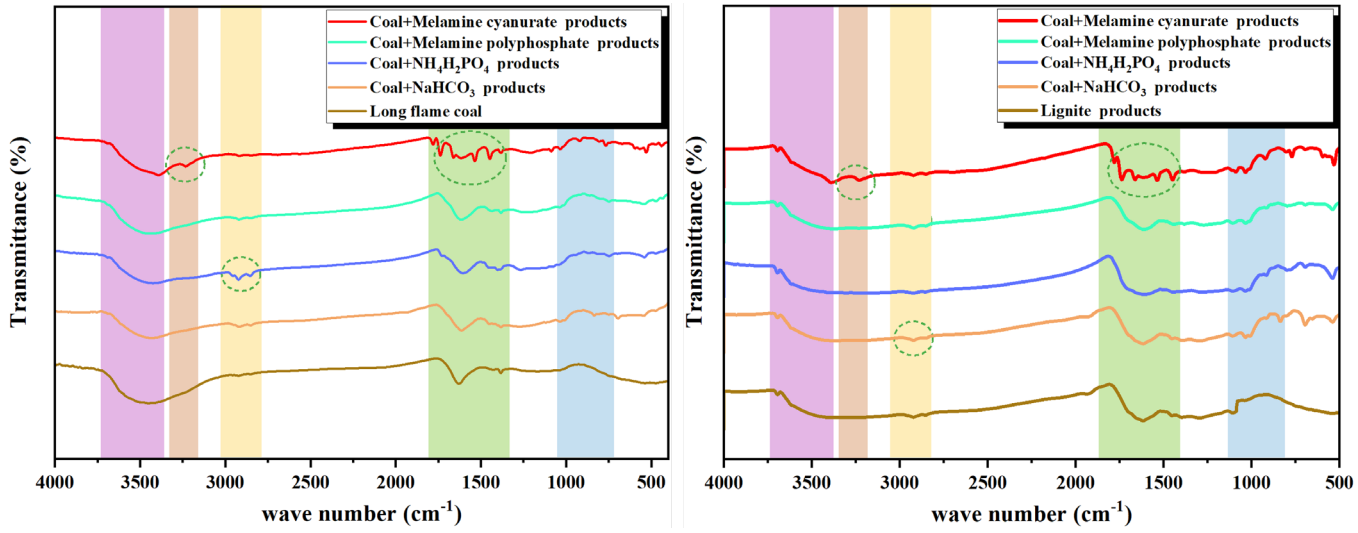

Figure 8. Infrared spectra of explosive products. The green dashed circle represents the absorption peak.

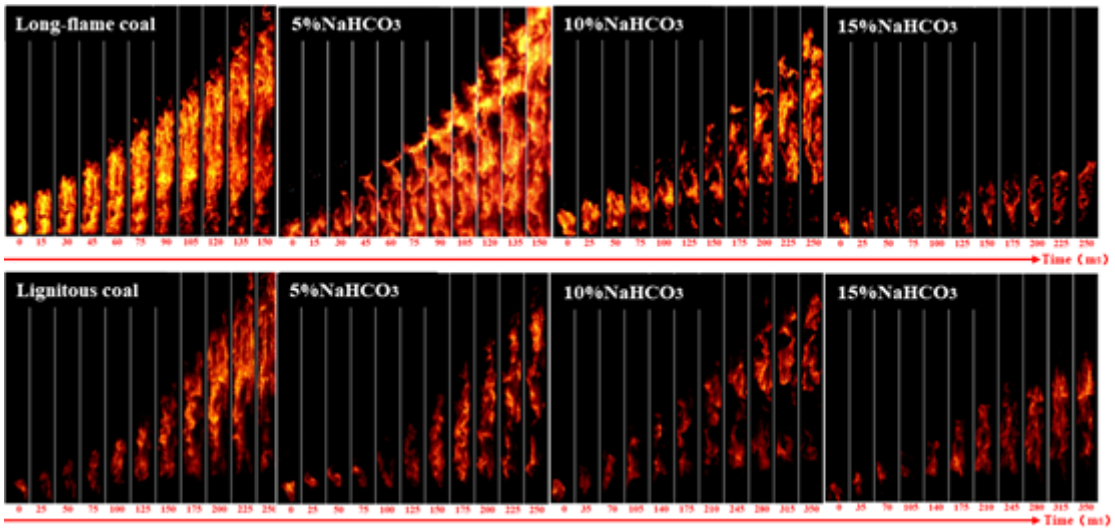

Figure 9. Flame propagation characteristics of adding $NaHCO_3$ to coal powder.

dispersed. The brightness has increased to a certain extent, mainly due to the production of dilution gases such as CO_2 after the heating reaction of $NaHCO_3$, resulting in more dispersed coal dust particles and poor flame suppression effect of trace explosion suppressants. With the continuous addition of $NaHCO_3$ explosion suppressant, the flame brightness significantly decreased and a slight fault appeared at the bottom after adding 10% explosion suppressant. After adding 15% explosion suppressant, the combustion of long-flame coal produces a trace flame that quickly extinguishes.

For brown coal, adding 5% $NaHCO_3$ reduced the brightness and propagation height of the brown coal flame, and discontinuous faults began to appear in the flame. After adding 10% $NaHCO_3$, the combustion flame faults become more obvious, and with the continuous addition of explosion suppressants, the flame intensity also decreases and the propagation height gradually decreases. Both the types of explosion suppressants effectively prevented the combustion reaction of coal powder; however after adding the same amount of explosion suppressant, $NaHCO_3$ had a more significant weakening effect on long-flame coal with better combustion efficiency.

As shown in Figure 10, after adding 5% $NH_4H_2PO_4$, the propagation time of long-flame coal increased from 150 ms to 400 ms with a significant fault phenomenon at the bottom of the pipeline. After adding 10% $NH_4H_2PO_4$, the time for the flame to reach its peak was extended to 450 ms, and the flame brightness gradually dimmed. The long-flame coal combustion flame only stayed at the ignition electrode, and the flame brightness and intensity were significantly reduced, producing a trace amount of flame that quickly extinguished. After adding 5% $NH_4H_2PO_4$, the flame brightness of long-flame coal significantly decreased, indicating that $NH_4H_2PO_4$ has a better inhibitory effect on long-flame coal than $NaHCO_3$. After adding 5% $NH_4H_2PO_4$, the flame brightness and propagation height of lignite decreased to a certain extent, and the flame did not propagate to the top of the pipeline. After adding 10% $NH_4H_2PO_4$, the flame distribution became more dispersed. After adding 15% $NH_4H_2PO_4$, the flame remains at the ignition electrode. After adding 15% $NH_4H_2PO_4$, the propagation time of long-flame coal increased from 150 ms to 400 ms, and the propagation time of brown coal increased from 250 ms to 300 ms. From the perspective of overall propagation time, $NH_4H_2PO_4$ has a better explosion suppression effect on long-flame coal.

From Figure 11, it can be seen that after adding 5% MCA, the propagation time of long-flame coal increased from 150 ms to 250 ms, and a fault phenomenon appeared at the bottom of the pipeline when the flame propagated to the top. After adding 10% MPP, the time for the flame to propagate to the farthest distance was extended again to 300 ms, and the flame brightness gradually decreased. The flame propagation height significantly decreased, and the coal dust flame was

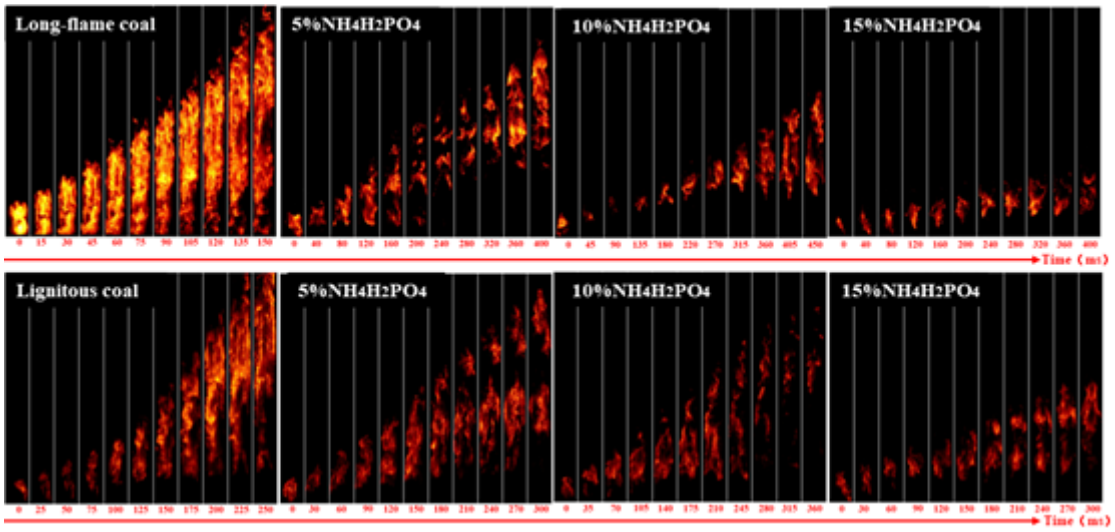

Figure 10. Flame propagation characteristics of adding $NH_4H_2PO_4$ to coal powder.

concentrated at the bottom of the pipeline. After adding 15% MCA, the flame became discrete. After adding 5% MCA, the flame propagation time of lignite to the farthest distance was extended to 300 ms. After adding 10% MCA, the flame distribution became more discrete, and long-distance faults appeared at the bottom. After adding 15% MCA, the flame exists in the form of a flame. The propagation time has also become 450 ms. After adding 15% MCA, the propagation time of long-flame coal increased from 150 ms to 400 ms, and the propagation time of lignite increased from 250 ms to 450 ms. From the overall propagation time, MCA has a better explosion suppression effect on long-flame coal. However, based on the analysis of flame dispersion and propagation distance, MCA has a weaker explosion suppression effect on long-flame coal. Therefore, the explosion suppression effect of MCA on the two types of coal is basically equivalent.

As shown in Figure 12, when 5% MPP is added, the propagation time of long-flame coal increases from 150 ms to 250 ms with the significant reduction in the flame brightness and height. After adding 10% MPP, the flame propagation time was shortened to 200 ms, and the flame brightness gradually decreased. After adding 15% MPP, flames were only generated at the ignition electrode and quickly extinguished for 50 ms, indicating complete suppression of long-flame coal. After adding 5% MPP to lignite, the flame did not reach the top of the pipeline, and a fault appeared at the bottom of the flame. It took 360 ms for the flame to spread to the farthest distance. After adding 10% MPP, the flame was basically extinguished, and a trace flame appeared with a propagation time of 500 ms. After adding 15% MPP, the flame only generated at the ignition electrode and quickly extinguished at 50 ms, indicating complete suppression of long-flame coal. Due to the complete suppression achieved by both types of coal at 15% MPP, compared to the flame morphology at 10% MPP, the flame propagation time of long-flame coal increased from 150 ms to 200 ms after the addition of 10% MPP, while that of lignite increased from 250 ms to 500 ms. Moreover, the flame brightness of lignite was weaker than that of long-flame coal after the addition of 10% MPP. Based on the comparison of time and flame morphology, it can be seen that the explosion suppression effect of MPP on lignite is due to the long-flame coal.

The above research indicates that different explosion suppressants have different explosion suppression effects on the same type of coal, and the same explosion suppressant also has different explosion suppression effects on two different types of coal. The above results indicate that $NaHCO_3$ and $NH_4H_2PO_4$ explosion suppressants have better explosion suppression effects on long-flame coal than lignite, MCA explosion suppressant has comparable explosion suppression effects on the two types of coal, and MPP has better explosion suppression effects on lignite than long-flame coal. After adding 15% of different explosion suppressants, MPP achieved complete suppression. Therefore,

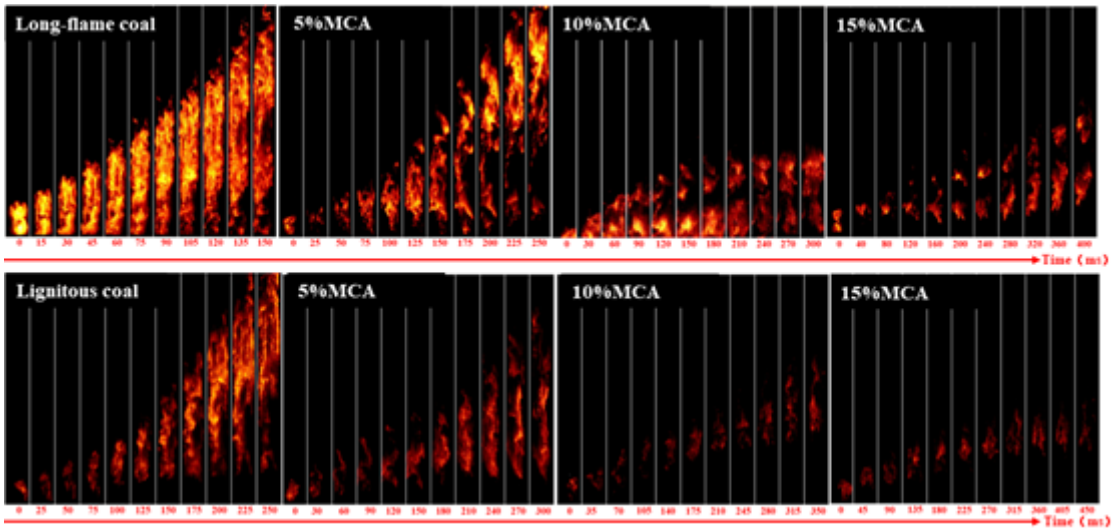

Figure 11. Flame propagation characteristics of adding melamine cyanurate (MCA) to coal powder.

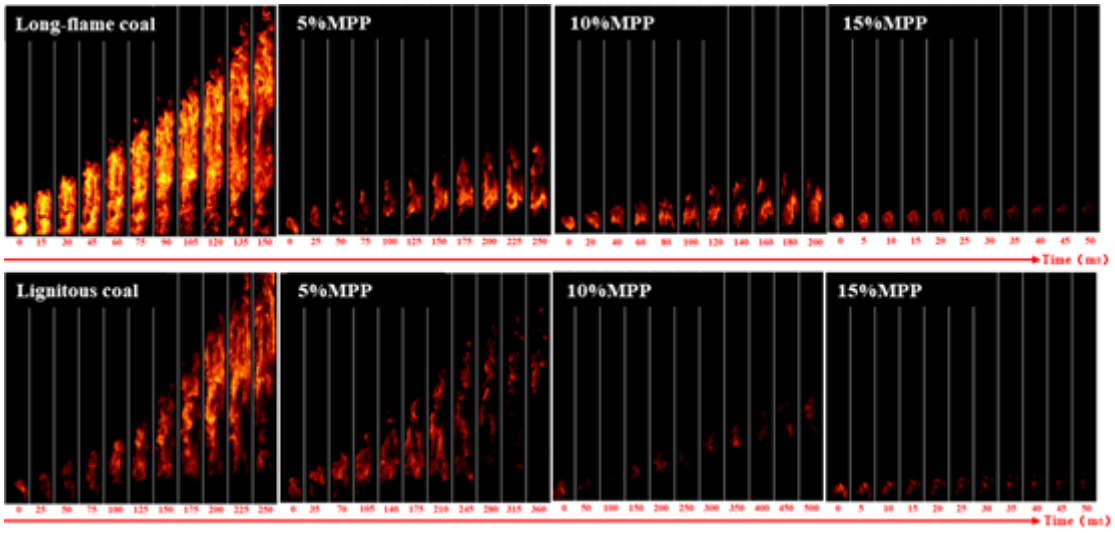

Figure 12. Flame propagation process of pulverized coal when melamine polyphosphate (MPP) is added.

the explosion suppression effect of MPP is better than the other three explosion suppressants. MPP has the best suppression effect on coal dust. After the addition of 5% of various explosion suppressants and the flame morphology of coal, $NaHCO_3$ has the worst suppression effect.

3.3.2 Analysis of coal powder flame propagation speed under different suppression conditions

The data on flame position and flame propagation speed are analyzed using video analysis software and image processing software. The flame front position and propagation speed of lignite and long-flame coal are shown in Figure 13. As shown in Figure 13(a) and Figure 13(b), before 110 ms, the flame front position of long-flame coal is higher than that of lignite, and after 110 ms, the flame height of lignite exceeds that of long-flame coal. However, from the overall development trend analysis, the change in the position of the flame front of long-flame coal is smoother, while the change in the position of the flame front of brown coal is greater in the later stage of combustion. There are four stages of flame propagation. At the beginning of ignition, the flame is constrained by the glass tube wall, resulting in pressure fluctuations during the propagation process. The flame is influenced by hot gas and turbulence and propagates upwards. Entering the next stage, the cooling effect of the flame on the pipeline wall affects the loss of some heat, and the flame weakens in a short period of time. Continuing to develop in the next stage, the flame emits more heat than it loses, and then accelerates upwards. In the final stage, the oxygen and fuel content is insufficient to support flame combustion, and the flame propagation process gradually ends.

The flame propagation speed is shown in Figure 14. According to Figure 14 (a), MPP has a good suppression effect on the propagation speed of brown coal detonation flames, with a V_{max} of only 0.25 m/s. $NaHCO_3$ has the worst suppression effect, with a V_{max} of 1.85 m/s. MCA and $NH_4H_2PO_4$ have similar suppression effects on V_{max}. When $NaHCO_3$ is added, the early flame height and speed are lower. For the entire combustion process, MPP has a better inhibitory effect than $NaHCO_3$, but in the initial stage of combustion, $NaHCO_3$ has a better effect. According to Figure 14 (b), MPP has the best suppression effect on the propagation speed of brown coal detonation flames, with a maximum flame propagation speed of only 0.28 m/s. MCA has the worst suppression effect, with a maximum flame propagation speed of about 1.4 m/s, followed by $NH_4H_2PO_4$ and $NaHCO_3$.

Comparing the effects of four inert materials on the propagation speed of two types of coal dust explosion flames, it can be concluded that MPP has the best suppression effect. After adding $NaHCO_3$ powder, the V_{max} decreased by 78.2% and 81.4%, respectively; after adding $NH_4H_2PO_4$, the V_{max} decreased by 87.2% and 87.9%. However, after adding MCA powder, the V_{max} decreased by 86.2% and 79.6%, respectively. The above analysis shows that $NaHCO_3$ and $NH_4H_2PO_4$ have better inhibitory effects on long-flame coal, MCA has better inhibitory effects on lignite, and MPP has the best inhibitory effect on the combustion process of the two types of coal dust.

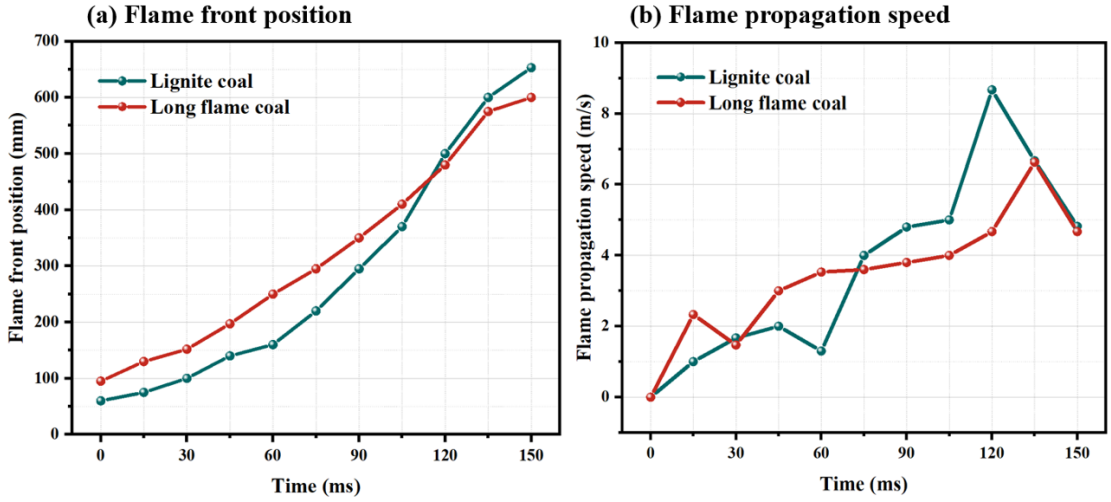

Figure 13. Image of flame front (a) Flame front position; (b) Flame propagation speed.

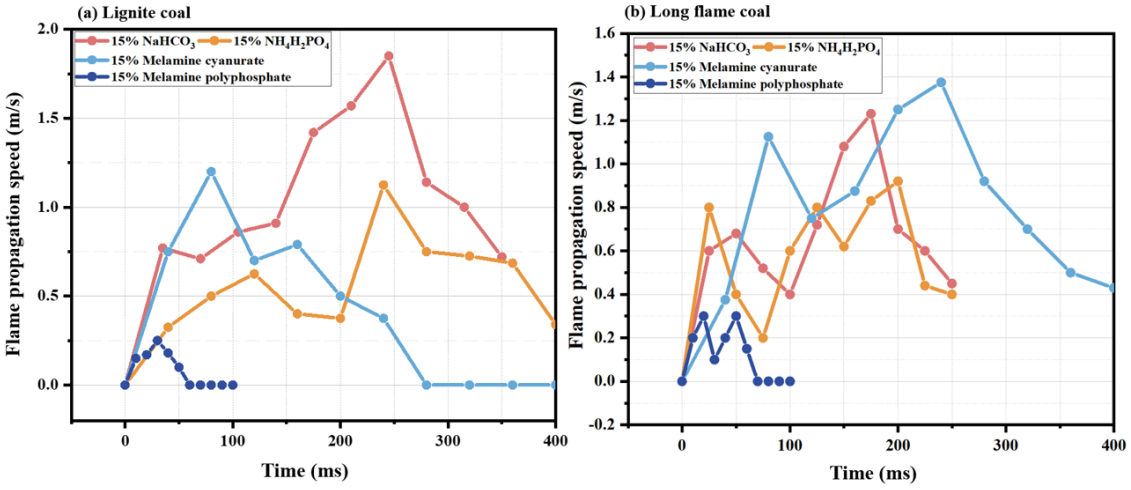

Figure 14. Effects of different chemical powder inhibitors on flame (a) Lignite coal; (b) Long flame coal.

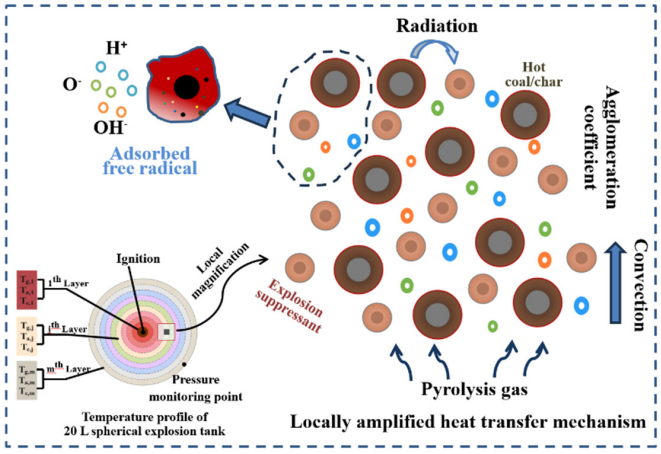

Figure. 15. Coal dust explosion mechanism.

3.4. Inhibition mechanism of explosion suppressants on coal dust

The mechanism of coal dust explosion is shown in Figure 15. When the heat from ignition acts on nearby coal particles, it initiates a pyrolysis process that releases volatile matter. When the combustible volatile matter reaches a sufficient concentration and mixes with air, rapid combustion reactions will occur. With the complete combustion of volatile matter, the residual fixed carbon in the semi coke will also begin to burn, generating a large amount of CO_2. There will be significant energy transfer between burnt and unburned coal dust, and strong energy exchange will stimulate the intense combustion of unburned coal dust. With the rapid spread and accumulation of combustion energy, the coal dust in the entire space will enter the combustion state comprehensively. In a sealed environment, the rapid increase in space temperature caused by combustion further promotes the expansion of gas volume, resulting in an instantaneous increase in pressure and triggering an explosion phenomenon. Explosion suppressant particles will be evenly dispersed around the hot coal and semi coke particles, effectively absorbing some of the heat released by them, gradually reducing the heat energy emitted to the external environment, and thereby inhibiting further combustion reactions of combustibles, forming a barrier for heat transfer. In addition, explosion suppressants consume high-energy free radicals such as O, OH, and H that promote combustion during the decomposition process, slowing down the speed of the entire combustion reaction, lowering the maximum temperature of the explosion, and interrupting the chain reaction process of the explosion, effectively suppressing the occurrence of the explosion.

4. Conclusions

This study uses four chemical powder explosion suppressants—$NaHCO_3$, $NH_4H_2PO_4$, MPP, and MCA—to select two types of coal dust with different degrees of metamorphism: long-flame coal and lignite. On analyzing the macroscopic parameters of the four chemical powder explosion suppressants under different inhibition conditions and combining with the characterization experiments of explosion residues, the explosion suppression performance of the chemical powder explosion suppressants on coal dust with different degrees of metamorphism is obtained. The main conclusions are as follows:

The difference in volatile matter content between the two types of coal powder exceeds 10%, but the difference in P_{max} is around 0.07 MPa. The difference in $(dP/dt)_{max}$ between the two is significant, indicating that $(dP/dt)_{max}$ is sensitive to volatile matter content. $NaHCO_3$ has a good inhibitory effect on the $(dP/dt)_{max}$ of lignite, but its inhibitory effect on P_{max} is minimal. And $NH_4H_2PO_4$, MCA, and MPP all have better inhibitory effects on the P_{max} of lignite.

The increase in inhibitor concentration will significantly reduce the brightness of the flame, weaken the continuity of the flame structure, and gradually slow down the upward trend of the flame front. Among different explosion suppressants, MPP achieved complete suppression after adding 15%, and exhibited the best explosion suppression effect. $NaHCO_3$ and $NH_4H_2PO_4$ explosion suppressants have better explosion suppression effects on long-flame coal than lignite, while MCA explosion suppressant has comparable explosion suppression effects on both types of coal.

After adding explosion suppressants, the surface of the residue becomes rougher and the pore structure is less developed. More inert substances are coated on the surface of coal dust. Functional groups such as NaOH, P-O-C, N-H, and - NH are involved in the coal dust explosion process and have a suppressive effect on the coal dust explosion.

Intense energy exchange occurs at the interface between burnt and unburned coal dust, triggering intense combustion of unburned coal dust. This combustion causes rapid gas expansion and a sudden pressure increase, leading to an explosion phenomenon. Cold explosion suppressant particles are evenly dispersed around hot coal/semi coke particles, serving to block heat transfer. Decomposition products from the explosion suppressants consume high-energy free radicals such as O, OH, and H, reducing the explosion temperature and the explosion chain reaction process.

CRediT authorship contribution statement

Yansong Zhang: Investigation, Methodology, Software, Writing–original draft, Writing – review & editing. **Yunkuan Zhang:** Conceptualization, Funding acquisition, Writing – review & editing. **XiangBao Meng:** Investigation, Project administration, Validation, Visualization. **Jie Zhang:** Conceptualization, Investigation. **Xiangrui Wei:** Formal analysis, Writing - review & editing. **Jing Shi:** Formal analysis, Methodology, Writing–review & editing.

Declaration of competing interest

The authors declare that they have no known competing financial interests or personal relationships that could have appeared to influence the work reported in this paper.

Acknowledgments

This work was supported by the National Natural Science Foundation of China (Grant No. 52404242) and China Postdoctoral Science Foundation (Grant No. 2024MD753981).

References

1. Bhattacharjee, R.M., Dash, A.K., Paul, P.S., 2020. A root cause failure analysis of coal dust explosion disaster – Gaps and lessons learnt. *Engineering Failure Analysis* **111**, 104229. https://doi.org/10.1016/j.engfailanal.2019.104229
2. Nie, B., Zhang, H., Liu, X., Peng, C., Hu, F., He, H., Bao, S., Zhou, H., Yang, T., 2024. Study on explosion characteristics and microstructure correlation analysis of coal dust in the presence of various concentrations and particle sizes. *Fuel* **373**, 132393. https://doi.org/10.1016/j.fuel.2024.132393
3. Wei, Q., Zhang, Y., Chen, K., Liu, B., Meng, X., Zhang, X., Chen, H., Chen, J., 2021. Preparation and performance of novel APP/NaY–Fe suppressant for coal dust explosion. *Journal of Loss Prevention in the Process Industries* **69**, 104374. https://doi.org/10.1016/j.jlp.2020.104374
4. Da, H., Yin, H., Liang, G., 2022. Explosion inhibition of coal dust clouds under coal gasification atmosphere by talc powder. *Process Safety and Environmental Protection* **165**, 286–294. https://doi.org/10.1016/j.psep.2022.07.021
5. Zhang, Y., Wu, G., Cai, L., Zhang, J., Wei, X., Wang, X., 2021b. Study on suppression of coal dust explosion by superfine NaHCO3/shell powder composite suppressant. *Powder Technology* **394**, 35–43. https://doi.org/10.1016/j.powtec.2021.08.037
6. Zhao, Q., Li, Y., Chen, X., 2022. Fire extinguishing and explosion suppression characteristics of explosion suppression system with N2/APP after methane/coal dust explosion. *Energy* **257**. https://doi.org/10.1016/j.energy.2022.124767
7. Lyu, X., Qiao, Y., Yuan, D., Zhang, Z., Zuo, W., Hua, J., Wang, Y., Zhang, L., 2024. Investigation and CFD simulation of coal dust explosion accident in confined space: A case study of Gaohe Coal Mine Ventilation Air Methane oxidation power plant. *Fire Safety Journal* **149**, 104237. https://doi.org/10.1016/j.firesaf.2024.104237
8. Wu, Y., Meng, X., Zhang, Y., Shi, L., Wu, Q., Liu, L., Wang, Z., Liu, J., Yan, K., Wang, T., 2023. Experimental study on the suppression of coal dust explosion by silica aerogel. *Energy* **267**, 126372. https://doi.org/10.1016/j.energy.2022.126372
9. Zhang, L., Wang, H., Chen, C., Wang, P., Xu, L., 2021. Experimental study to assess the explosion hazard of CH4/coal dust mixtures induced by high-temperature source surface. *Process Safety and Environmental Protection* **154**, 60–71. https://doi.org/10.1016/j.psep.2021.08.005

10. Tan, B., Shao, Z., Xu, B., Wei, H., Wang, T., 2020. Analysis of explosion pressure and residual gas characteristics of micro-nano coal dust in confined space. *Journal of Loss Prevention in the Process Industries* **64**, 104056. https://doi.org/10.1016/j.jlp.2020.104056
11. Wang, H., Zhang, Y., Tian, S., Hu, Y., Xu, J., 2024. Experimental study on characteristics of methane-coal dust explosions and the spatiotemporal evolution of flow field in early flame. *Case studies Thermal Engineering* **61**, 104978. https://doi.org/10.1016/j.csite.2024.104978
12. Wang, X., Zhang, Yansong, Liu, B., Liang, P., Zhang, Yaqing, 2019. Effectiveness and mechanism of carbamide/fly ash cenosphere with bilayer spherical shell structure as explosion suppressant of coal dust. *Journal of Hazardous Materials* **365**, 555–564. https://doi.org/10.1016/j.jhazmat.2018.11.044
13. Proust, C., 2006. A few fundamental aspects about ignition and flame propagation in dust clouds. *Journal of Loss Prevention in the Process Industries* **19**, 104–120. https://doi.org/10.1016/j.jlp.2005.06.035
14. Cao, W., Huang, L., Zhang, J., Xu, S., Qiu, S., Pan, F., 2012. Research on characteristic parameters of coal-dust explosion. *Procedia Engineering* **45**, 442–447. https://doi.org/10.1016/j.proeng.2012.08.183
15. Zubov, V.P., Golubev, D.D., 2021. Prospects for the use of modern technological solutions in the flat-lying coal seams development, taking into account the danger of the formation of the places of its spontaneous combustion. *Journal of Mining Institute*. **250**, 534–541. https://doi.org/10.31897/PMI.2021.4.6
16. Tao, W., Jiang, B., Zheng, Y., Lu, K., Ji, B., Wang, X.H., Yu, C.F., Zhou, G., Sun, B., Wang, J., 2024. Effect of alkyl glycoside surfactant on the explosion characteristics of bituminous coal: Experimental and theoretical discussion. *Energy* **288**, 129930. https://doi.org/10.1016/j.energy.2023.129930
17. Yin, H., Dai, H., Liang, G., 2022. Inhibition evaluation of magnesium hydroxide, aluminum hydroxide, and hydrotalcite on the flame propagation of coal dust. *Process Safety and Environmental Protection* **157**, 443–457. https://doi.org/10.1016/j.psep.2021.11.048
18. Lu, K., Jiang, B., Xiao, Y., Luo, Z., Chen, X., Zhao, Y., Wang, Y., 2024. Study on inhibiting effects of melamine polyphosphate on pulverized coal explosion: Investigation from macro and micro perspectives. *Fuel* **360**, 130574. https://doi.org/10.1016/j.fuel.2023.130574
19. Dai, H., Yin, H., Zhai, C., 2022. Experimental investigation on the inhibition of coal dust deflagration by the composite inhibitor of floating bead and melamine cyanurate. *Energy* **261**. https://doi.org/10.1016/j.energy.2022.125207
20. Chen, K., Zhang, Y., Zhang, P., Li, L., Chen, J., Pan, Z., Li, R., He, M., 2022. Study on the preparation of green suppressors and their characteristics in coal dust flame propagation inhibition. *Advanced Powder Technology* **33**. https://doi.org/10.1016/j.apt.2022.103749
21. Jiang, H., Bi, M., Gao, W., 2022. In situ analysis of suppression mechanism of DMMP water mist in coal dust explosions using pyrolysis time-of-flight mass spectrometry. *Chemical Engineering Science* **260**, 117836. https://doi.org/10.1016/j.ces.2022.117836
22. Wei, X., Zhang, Yansong, Wu, G., Zhang, X., Zhang, Yaqing, Wang, X., 2021. Study on explosion suppression of coal dust with different particle size by shell powder and $NaHCO_3$. *Fuel* **306**, 121709. https://doi.org/10.1016/j.fuel.2021.121709
23. Ren, X., Zhang, J., Jia, H., 2024. Influence of sodium hydrogen carbonate, ammonium dihydrogen phosphate, and lignin-based explosion inhibitors on the sensitivity of coal dust explosion. *Process Safety and Environmental Protection* **189**, 1193–1206. https://doi.org/10.1016/j.psep.2024.07.014
24. Sun, S., Peng, H., Pang, L., Zhao, H., Li, Y., 2024. Establishment of a model for NaHCO3 inhibition of coal dust explosions and molecular dynamics experimental study. *Fuel* **358**, 130150. https://doi.org/10.1016/j.fuel.2023.130150
25. Zhang, Yansong, Zhang, Youning, Shi, J., Cao, M., Wei, X., Shi, L., Wang, X., 2024. Experimental and numerical study on suppressing coal dust deflagration flame with $NaHCO_3$ and MPP. *Fuel* **358**, 130152. https://doi.org/10.1016/j.fuel.2023.130152
26. Zhang, Y., Chen, K., Yang, J., Chen, J., Pan, Z., Shi, W., Meng, X., Zhang, X., He, M., 2021a. The Performance and Mechanism of the Green Explosion Suppressant SGA for Coal Dust Explosion Suppression. *ACS Omega* **6**, 35416–35426. https://doi.org/10.1021/acsomega.1c04791
27. Yan, K., Qi, S., Li, R., Sun, H., Bai, J., Wang, K., Li, M., Yuan, M., 2024. Study on the inhibition of explosion and combustion of coal dust based on the structure of core-shell microencapsulated polyurethane. *Energy* **290**, 130159. https://doi.org/10.1016/j.energy.2023.130159
28. Zhao, F., Gao, W., Jiang, H., Jin, S., Zhang, Z., Nie, Z., 2024. Inhibition mechanism of phosphorus-containing inhibitor on coal dust pyrolysis during explosions using in-situ Py-TOF-MS. *Chemical Engineering Science* **293**, 120072. https://doi.org/10.1016/j.ces.2024.120072
29. Li, Y., Meng, X., Song, S., Chen, J., Ding, J., Yu, X., Zhu, Y., Qin, Z., 2024. Piperazine pyrophosphate-functionalized Ni-MOF metal framework: Fabrication and synergistic explosion suppression mechanisms. *Chemical Engineering Journal* **499**, 155870. https://doi.org/10.1016/j.cej.2024.155870
30. Yu, X., Meng, X., Chen, J., Zhu, Y., Li, Y., Qin, Z., Ding, J., Song, S., 2024. Macroscopic behavior and kinetic mechanism of ammonium dihydrogen phosphate for suppressing polyethylene dust deflagration. *Chemical Engineering Journal* **498**, 155320. https://doi.org/10.1016/j.cej.2024.155320
31. Qin, X., Zhang, Y., Shi, J., Wei, X., 2024. Study on Explosion Characteristics and Mechanism of Electrostatic Spray Powder. *ACS Omega* **9**, 19645–19656. https://doi.org/10.1021/acsomega.4c01724
32. Qin, X., Wei, X., Shi, J., Yan, Y., Zhang, Y., 2023. Research on the Inhibition Effect of NaCl on the Explosion of Mg-Al Alloy Powder. *ACS Omega*. https://doi.org/10.1021/acsomega.3c08242